Applied Catalysis B: Environmental 162 (2015) 327–337

Contents lists available at ScienceDirect

Applied Catalysis B: Environmental

journal homepage: www.elsevier.com/locate/apcatb

A comprehensive study on Pt/Al_2O_3 granular catalyst used for sulfuric acid decomposition step in sulfur–iodine thermochemical cycle: Changes in catalyst structure, morphology and metal-support interaction

A.M. Banerjee[a], M.R. Pai[a], R. Tewari[b], Naina Raje[c], A.K. Tripathi[a], S.R. Bharadwaj[a,*], D. Das[a]

[a] Chemistry Division, Bhabha Atomic Research Centre, Mumbai 400085, India
[b] Material Science Division, Bhabha Atomic Research Centre, Mumbai 400085, India
[c] Analytical Chemistry Division Bhabha Atomic Research Centre, Mumbai 400085, India

ARTICLE INFO

Article history:
Received 6 May 2014
Received in revised form 26 June 2014
Accepted 3 July 2014
Available online 9 July 2014

Keywords:
Sulfuric acid decomposition
Pt/Al_2O_3
Granular catalyst
Sulfated alumina
Metal-support interaction

ABSTRACT

In continuation with our last communication on granular Fe_2O_3 catalysts (Banerjee et al., Applied Catalysis B: Environmental 127 (2012) 36–46), we report here a thorough investigations on Pt/Al_2O_3 catalyst in granular form of 4–6 mm diameter for sulfuric acid decomposition reaction in absence of any carrier or diluents gas in a dual tube quartz catalytic reactor, which served as an integrated boiler, preheater and catalytic decomposer. SO_2 yield were evaluated as a function of reaction variables e.g. time, temperature and sulfuric acid flux for Pt/Al_2O_3 catalyst and compared with earlier results obtained with Fe_2O_3 based catalysts. The SO_2 yield increased as a function of temperature while it decreased with an increase in sulfuric acid flux. A decrease in SO_2 yield from 80% to 73% was observed for Pt/Al_2O_3 catalyst during a 100 h run at 800 °C and at an acid flux of 0.63 ml min^{-1} (WHSV of ~3.4 g acid g^{-1} h^{-1}). To determine the cause of this deactivation, both the fresh and spent catalysts were characterized for structure and morphology by ICP-AES, N_2-adsorption desorption isotherm, pulsed chemisorption of H_2, XRD, FTIR, SEM, TEM and HR-TEM. The support alumina underwent major physicochemical changes on prolonged use under the harsh reaction conditions at elevated temperatures viz. reduction in porosity and surface area, sulfation, and partial phase transformation. On the other hand, the active metal Pt, which exhibited a small and narrow particle size distribution and good dispersion in the fresh catalyst, suffered thermal sintering on long term use to form large agglomerates with a non-uniform size distribution and poor dispersion. An attempt was made to understand the existence of any metal-support interaction by recording the TG-DTG-evolved gas analysis of the spent catalyst and comparing it with the thermal properties of bulk aluminum sulfate. The thermal investigations revealed that a synergistic effect existed between the Pt-particles and the sulfated alumina support.

© 2014 Elsevier B.V. All rights reserved.

1. Introduction

Thermochemical cycles for hydrogen generation from water consist of a series of chemical reactions which split water to produce hydrogen and oxygen separately at much lower temperatures than required for the direct thermal decomposition of water [1–4]. The primary energy source to drive the cycle can be provided either by nuclear [4,5] or solar heat [4,6]. The sulfur based thermochemical cycles e.g. the sulfur–iodine thermochemical cycle [4–6] and the hybrid sulfur cycle [7] are promising ones by virtue of their higher efficiencies and feasibility [4,7–9]. In these cycles sulfuric acid decomposition reaction is utilized as the highest temperature step to derive heat from the nuclear reactors or solar concentrators. The development of stable and active catalyst for sulfuric acid decomposition is a crucial aspect in successful and efficient operation of the sulfur based thermochemical cycles.

* Corresponding author. Head, Fuel Cell Materials and Catalysis Section, Chemistry Division, Bhabha Atomic Research Centre, Mumbai-400085.Tel.: +91 22 25595100; fax: +9122 25505151.
E-mail addresses: shyamala@barc.gov.in, shyamala27@hotmail.com (S.R. Bharadwaj).

http://dx.doi.org/10.1016/j.apcatb.2014.07.008
0926-3373/© 2014 Elsevier B.V. All rights reserved.

Decomposition of sulfuric acid the high temperature reaction in the sulfur based thermochemical cycles can be represented as:

$$H_2SO_4(g) \leftrightarrow H_2O(g) + SO_3(g)(\sim 450\,^{\circ}C) \quad (1)$$

$$SO_3(g) \leftrightarrow SO_2(g) + 0.5O_2(g)(\sim 800\text{–}900\,^{\circ}C) \quad (2)$$

Sulfuric acid can be decomposed to its anhydride SO_3 (Eq. (1)) with or without a catalyst, but the decomposition of SO_3 is a catalytic reaction (Eq. (2)) as the kinetics of this reaction is extremely slow at the desired temperatures of 800 °C to 900 °C. The catalyst efficiency, lifetime and cost play a significant role in determining the overall efficiency and cost of the hydrogen production process [10,11]. Two classes of catalyst-oxide based and supported noble metals, have been investigated for the above reaction, with each class having their own advantages and disadvantages.

We have earlier carried out detailed investigations with iron oxide based catalysts, where we have shown their effectiveness (chemical and thermal stability and high catalytic activity) for decomposition of sulfuric acid both in powder form at a small scale [12,13] and in granular form at an enhanced scale [14]. Besides, other groups have also reported the performance of various oxides, mixed metal oxides and supported oxide based catalysts for the above reaction [15–23].

On the other hand, supported noble metal, which is the more conventional class of heterogeneous catalyst and widely used in several industrial applications [24–26] has also been explored as a catalyst for the above reaction viz. Pt/ZrO_2, Pt/TiO_2, $Pt/BaSO_4$ and $Pt/A1_2O_3$ [27] by Norman et al; Pt/Al_2O_3, Pt/TiO_2 and Pt/ZrO_2 [28] by Ginosar et al; Pt/TiO_2 (rutile) [29] by Petkovic et al; ($Pt/BaSO_4$) [30] by Nagaraja et al; Pt/SiC coated Al_2O_3 catalyst [31] by Lee et al. and a theoretical study of metal particles – Pd, Pt, Rh, Ir, and Ru supported on TiO_2 [32] by Rashkeev et al. Even, in the demonstration studies on a closed-cycle hydrogen production by the thermochemical water-splitting iodine–sulfur process, JAERI mentions about the use of a "catalyst bed of platinum" [5]. Pt based catalysts were found to be active in all the above reports but some of them raised concerns regarding its stability. Loss of activity on long term use (200 h), primarily due to a loss in active metal Pt, was reported by Ginosar et al. [28]. Loss of catalytic activity of Pt/TiO_2 on loss of active metal was also encountered by Petkovic et al. [29] along with substrate sulfation but such sulfation did not apparently seem to be detrimental to the catalytic activity. On the other hand, loss in activity of Pt/Al_2O_3 catalyst due to substrate sulfation was reported by Norman et al. [27] and also by Lee et al. [31] (at temperatures below 750 °C). Again, sintering of the active component Pt and the substrate was also observed in the above reports; however a quantitative estimate regarding the extent of sintering by recording the high resolution transmission electron microscopy images is not available. So, more clarity is desirable on the effect of substrate sulfation on catalytic activity and the extent of sintering of the active metal due to long term use at high temperatures and its consequent effect on catalytic activity. Besides, in the above reports either the catalysts were employed in powder form, or in small amounts and carrier gas was employed to carry the sulfuric acid vapors over the catalyst.

So, to investigate and clearly establish the catalytic activity and stability of Pt-based catalyst for sulfuric acid decomposition, a commercial Pt (~0.5 wt. %)/Al_2O_3 catalyst was evaluated for the above reaction as a function of temperature (700 °C–825 °C), flux of sulfuric acid (0.2–3.5 ml min^{-1}) and time (100 h). Moreover, from a practical application approach, we employed 20 g of Pt/Al_2O_3 catalyst in granular form, 4–6 mm in diameter, in absence of any carrier gas or diluents, under the flow of vapors of concentrated sulfuric acid (~98%) alone. The conditions were kept similar to our earlier studies with iron oxide and 10% chromium doped iron oxide catalysts [14], so that a suitable comparison of the performance of Pt/Al_2O_3 can be made with the iron oxide based catalysts. In the present study both fresh and spent catalysts were characterized in details employing various techniques such as BET surface area measurement, hydrogen chemisorption, x-ray powder diffraction, Fourier Transform Infrared Spectroscopy, SEM-EDX, TEM, TG-IR to look deeper in to the above mentioned issues associated with the supported Pt-catalysts. An attempt is also made to delineate the role of metal and that of support during acid decomposition process by thermal analysis of the spent sample.

2. Experimental

2.1. Commercial Pt/Al_2O_3 catalyst

A commercial Pt (0.5 wt. %)/Al_2O_3 (procured from M/s. Manilal Maganlal & Co., Mumbai, India) granular sample of 4-6 mm diameter were characterized before and after 100 h use by various techniques. The as obtained catalyst was reduced using a gas mixture of 5% H_2 in N_2 at a flow rate of 60 ml min^{-1} at 350 °C for 2 h, and then cooled under N_2 flow prior to activity measurement.

2.2. Fresh and spent catalyst characterization

Throughout the manuscript we refer to the reduced Pt/Al_2O_3 sample as the fresh catalyst and the catalyst collected after a 100 h experimental run for sulfuric acid decomposition at 800 °C at a WHSV of 3.4 g acid g^{-1} catalyst h^{-1} as the spent or used catalyst. The Pt content of both the fresh and spent catalyst was evaluated using ICP-AES technique after microwave digestion of the powders (obtained by grinding the granules) in conc. HNO_3–HCl (aqua regia). The powder XRD patterns were recorded on a Philips X'Pert pro x-ray diffractometer using Cu K_α radiation (λ = 1.5418 Å) at 40 kV and 30 mA. A Quantachrome Autosorb-1 analyzer was employed for measurement of BET surface area by recording the nitrogen adsorption isotherms. The FTIR spectra of the solid samples were recorded in KBr using a Jasco FTIR (model 610) in range of 400-4000 cm^{-1} with a resolution of 4 cm^{-1}. The percent metal dispersion was evaluated by pulsed chemisorptions technique, applying measured doses of hydrogen gas over a fixed amount of the sample using a TPDRO analyzer (Thermoquest, Italy). The sample prior to chemisorptions measurements was pretreated at 350 °C first in hydrogen for 2 h, to reduce platinum completely and then in argon for 1 h. The morphological features were analyzed by a Scanning Electron Microscope (Mirero, Korea, model - AIS2100) and Energy Dispersive x-Ray spectroscopy (EDX). Low resolution transmission electron microscopy (TEM) images along with Energy Dispersive X-Ray Spectroscopy (EDX) were collected with a Philips CM 200 microscope operating at an accelerating voltage of 200 kV. High resolution TEM (HR-TEM) images were taken with a FEI-Tecnai G-20 microscope operating at 200 kV. The Thermo-gravimetry–evolved gas analysis (FTIR) were carried out in a Netzsch Thermobalance (Model No.: STA 409 PC Luxx) coupled to Bruker FTIR system (Model No.: Tensor 27) via a heated Teflon capillary (1 m long, 2 mm i.d.).

2.3. Catalytic activity measurements

The catalytic properties of spherical granules of Pt/Al_2O_3 samples were evaluated under flow through conditions in a dual tube quartz catalytic reactor with annular configuration as shown in Fig. 1 and explained in details elsewhere [14]. Briefly, sulfuric acid (~98 wt. %, AR Grade) was allowed to accumulate at the bottom of the annular region of the dual tube quartz catalytic reactor and 20 g of Pt/Al_2O_3 granules (4–6 mm) were placed at the top of the annular region, held on its position by a perforated quartz disc. The acid zone and the catalyst zone were heated separately by a

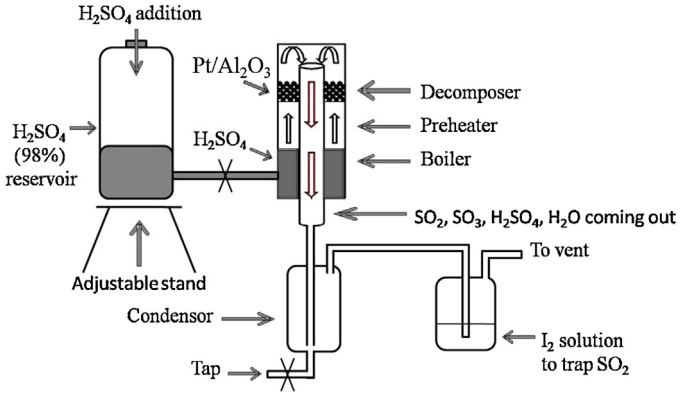

Fig. 1. Block diagram of the dual tube quartz experimental set up for carrying out sulfuric acid decomposition reaction with 20 g granular Pt/Al_2O_3 catalyst. The annular space in dual quartz tube reactor serves as the integrated boiler, preheater and catalytic decomposer [14].

two-temperature zone electric furnace while temperatures of the two zones were controlled by the thermocouples held on the outer surface of the quartz reactor. The region in between the acid zone and catalyst zone acted as a pre-heater region, where temperature increased gradually from the former to later zone, minimizing acid condensation. The catalytic activity were evaluated in the reactor as a function of temperature (700 °C–825 °C), time (100 h) at a sulfuric acid flux 0.63 ml min^{-1} (WHSV of 3.4 g acid g^{-1} catalyst h^{-1}) and as a function of flux of liquid sulfuric acid in the range of 0.2–3.5 ml min^{-1}. The product analysis was done by chemical titrimetric method [14], the unreacted acid being titrated after condensation and SO_2 was quantified by trapping it in iodine solution.

3. Results

3.1. Catalytic activity

The temperature dependent catalytic activity of the Pt/Al_2O_3 granules employed in the dual quartz tube catalytic reactor at a WHSV of ~3.4 g acid g^{-1} h^{-1} (flux of 0.63 ml min^{-1} of liquid sulfuric acid over 20 g of catalyst bed) is shown in Fig. 2A. The SO_2 yield increased with the increase in temperature with the maximum reaching to ~83% at 825 °C. For the sake of comparison the catalytic activities of both Fe_2O_3 and $Fe_{1.8}Cr_{0.2}O_3$ granules are also shown in the Fig. 2A [14]. We can see from Fig. 2A that the temperature dependent catalytic activity of Pt/Al_2O_3 granules is almost similar to $Fe_{1.8}Cr_{0.2}O_3$ granules, which was the most active catalyst as per our previous studies [12–14].

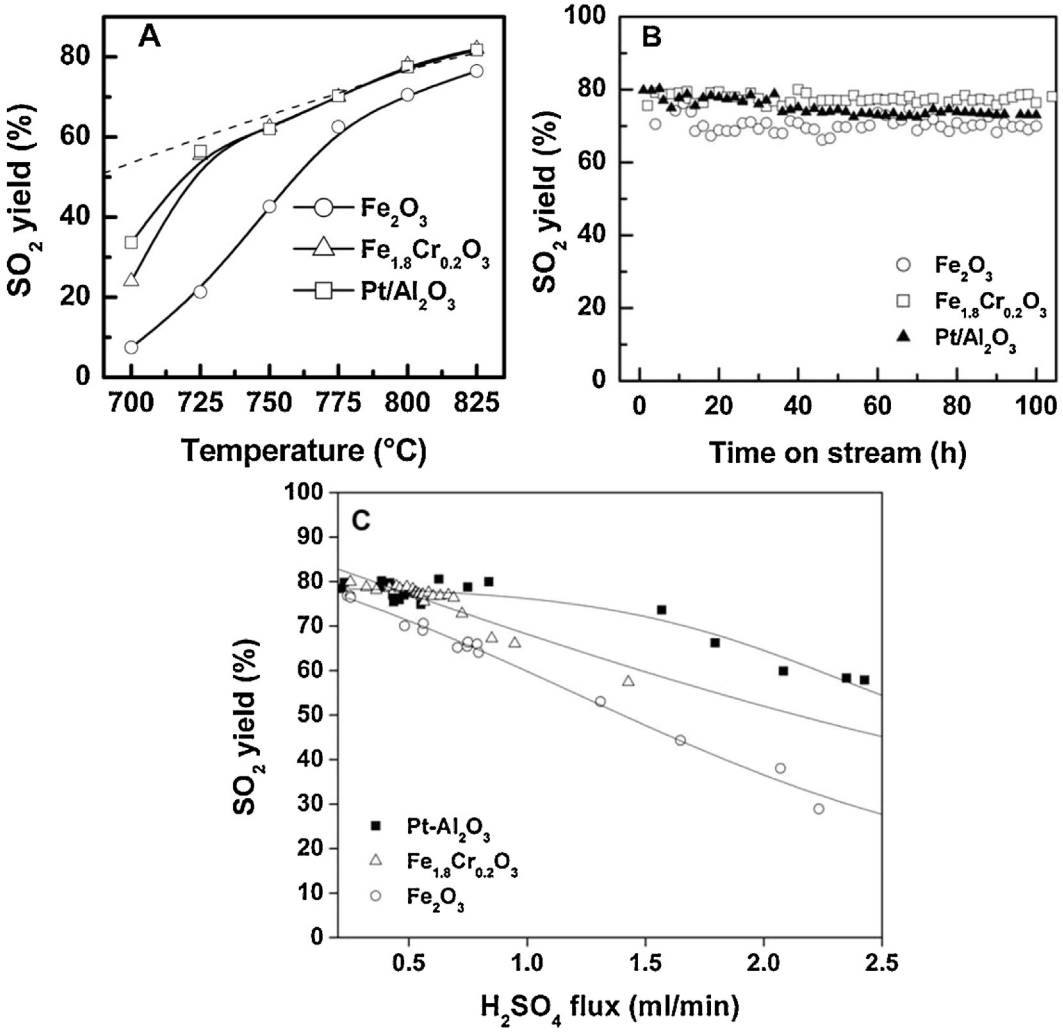

Fig. 2. Comparison of catalytic performance of granules (4–6 mm diameter) of Pt/Al_2O_3 with Fe_2O_3 and $Fe_{1.8}Cr_{0.2}O_3$ for sulfuric acid decomposition with 20 g catalyst in the dual quartz tube integrated boiler, preheater and decomposer. (A) Temperature dependent catalytic activity at WHSV of 3.4 g acid g^{-1} catalyst h^{-1} (acid flux 0.63 ml min^{-1}). The dashed curve represents thermodynamic yield (B) catalytic activity with respect to time on stream for 100 h at 800 °C with WHSV of 3.4 g acid g^{-1} catalyst h^{-1}(acid flux 0.63 ml min^{-1}) and (C) catalytic activity as a function of flux of sulfuric acid from 0.2 to 2.5 ml min^{-1} at 800 °C.

Table 1
Characteristics of the fresh and used Pt/Al_2O_3 catalysts.

Sample	Pt metal content	BET surface area	Pore volume	H_2 uptake	Dispersion
	Wt %	$m^2\,g^{-1}$	$cm^3\,g^{-1}$	$\mu mol\,g^{-1}$	
Fresh Pt/Al_2O_3	0.47	261	0.3615	17.2	0.71
Used Pt/Al_2O_3	0.44	145	0.1559	6 0.3	0.01

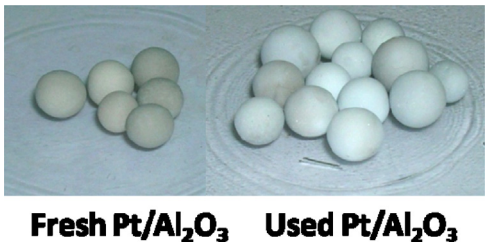

Fig. 3. Photograph of the fresh and spent (used) catalyst granules.

Results on long-term stability evaluation of the catalyst for 100 h run at 800 °C at a sulfuric acid flux of 0.63 ml min^{-1} (WHSV of ~3.4 g acid $g^{-1}\,h^{-1}$) are shown in Fig. 2 B. Contrary to the results obtained for the iron oxide based catalysts in our earlier work [14], the Pt-catalysts showed a decrease in activity during prolonged use. SO_2 yield decreased from ~80% to ~73% during 100 h run. But, in the case of the oxide catalysts any such decrease in catalytic activity was not noticed during the 100 h run at 800 °C [14].

The catalytic activity as a function of flux rate of sulfuric acid was also carried out at 800 °C and is shown in Fig. 2C.

We also carried out sulfuric acid decomposition in absence of active metal Pt, with support γ-Al_2O_3 pellets of 4–6 mm and we achieved a conversion of ~4% SO_2 yield at 800 °C at a sulfuric acid flux of 0.63 ml min^{-1} (WHSV of ~3.4 g acid $g^{-1}\,h^{-1}$), which is close to that obtained by Tagawa et al. [33].

The fresh Pt (~0.5 wt. %)/Al_2O_3 catalyst before carrying out the catalysis experiments was characterized for composition, structure and morphology by various techniques. The catalyst after 100 h use was collected and also well characterized *ex-situ*. The results were compared to analyze the physicochemical changes occurring to the Pt/Al_2O_3 sample on prolonged use under the corrosive reaction conditions at elevated temperatures.

3.2. Fresh and spent catalyst characterization

Fig. 3 shows the photograph of the fresh and the spent catalyst samples.

3.2.1. Pt-content, dispersion and surface area

Table 1 summarizes the results obtained for metal loading (ICP-AES), BET-surface area, pore volume, H_2-uptake (pulsed chemisorption) for the fresh and the spent Pt (~0.5 wt. %)/Al_2O_3 catalyst. The commercial catalyst was found to have a Pt-metal loading of 0.47 wt. % and on catalytic use for more than 100 h for sulfuric acid decomposition there was a decrease in metal content to 0.44 wt. %. Thus, we do not observe any substantial loss in Pt content as observed by other authors [28,29]. The BET-surface area of the fresh catalyst was 261 $m^2\,g^{-1}$ and after 100 h use the surface area decreased to 145 $m^2\,g^{-1}$. Reduction in BET surface area could possibly be due to sintering/modification of the alumina support during prolonged use of the catalyst. The fresh catalyst shows a hydrogen uptake of 17.2 $\mu mol\,g^{-1}$ in pulsed chemisorptions experiments, which corresponds to a very good dispersion of 71% (H/Pt = 1). The value decreases abruptly in the spent catalyst. Although, there is minimal volatilization of the Pt metal during long term use but there is a significant decrease in dispersion of the active metal.

3.2.2. N_2-adsorption desorption isotherm

The adsorption–desorption isotherms for the fresh and the spent catalyst are shown in Fig. 4. The fresh catalyst shows a Type IV isotherm generally encountered for mesoporous samples, which indicates the mesoporous nature of the alumina support of the fresh catalyst. The hysteresis implies the presence of cylindrical pores. Significant change in the porosity occurs due to catalytic use for 100 h at 800 °C, with the spent catalyst showing a major change in the adsorption-desorption isotherm (Fig. 4). The isotherm for the spent catalyst is convex type but not completely convex throughout which is generally encountered for non-porous

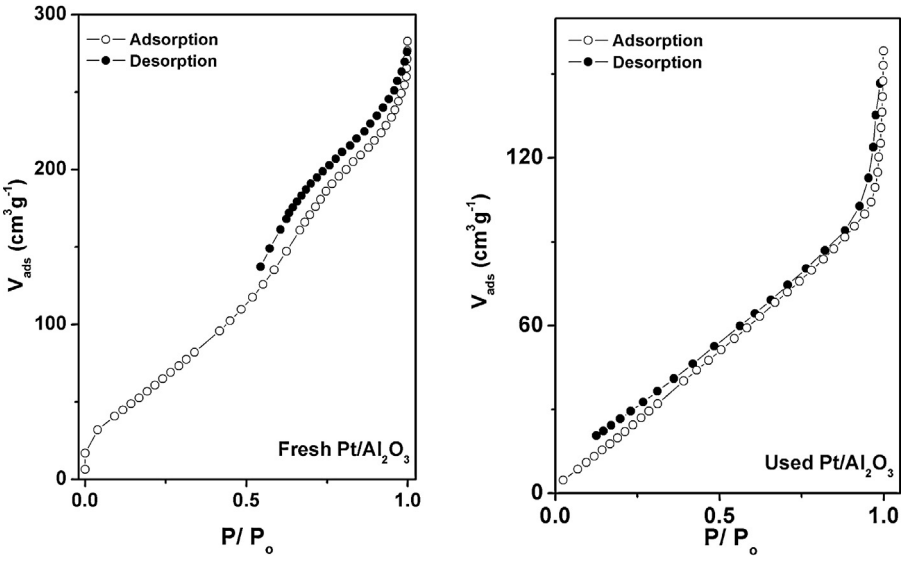

Fig. 4. Adsorption-Desorption isotherms for the fresh and the spent Pt/Al_2O_3 catalyst.

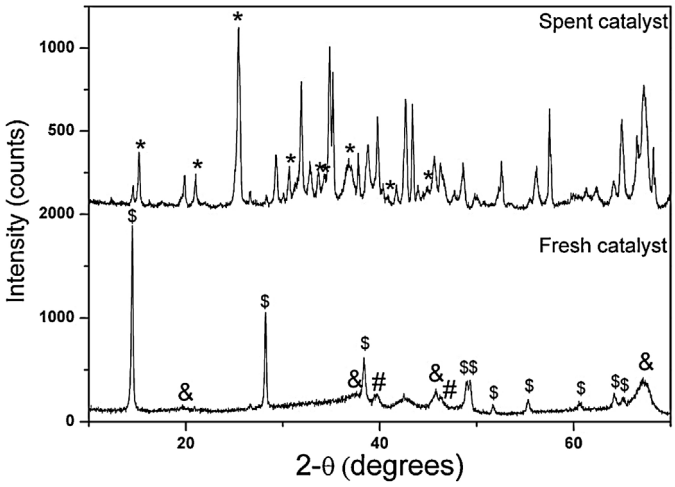

Fig. 5. Powder XRD patterns of the fresh and spent Pt/Al_2O_3 catalyst $ - AlO(OH) phase; & - γ-Al_2O_3 phase; # - Pt phase; * - $Al_2(SO_4)_3$ phase.

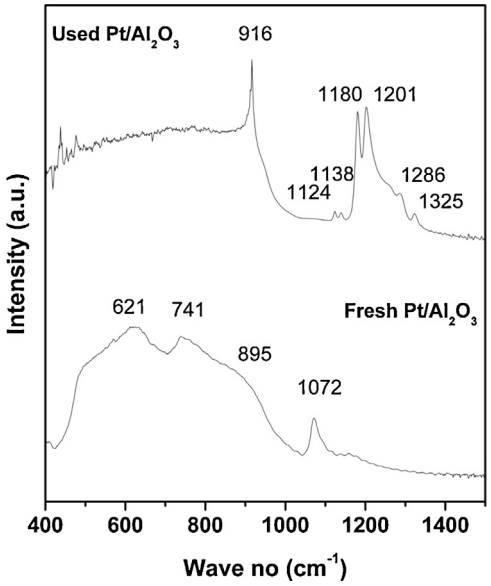

Fig. 6. FTIR spectra of the fresh and spent Pt/Al_2O_3 catalyst.

or macroporous solids with weak adsorptions. Also hysteresis in the adsorption–desorption isotherm is absent. These results definitely indicate a reduction in porosity of the support alumina which is further supported by the observation of the decrease in surface area and pore volume. The decrease in porosity can be attributed to sintering on high temperature use or even formation of newer species (viz. sulfates) or a change in crystalline phase of alumina.

3.2.3. Phase characterization by powder XRD

Fig. 5 shows the powder X-ray diffraction pattern of the fresh and the used Pt/Al_2O_3 catalyst. The fresh sample consists mainly of three phases – AlO(OH) phase (JCPDS card No. 211307) peak position marked by "$", γ-Al_2O_3 phase (JCPDS card No. 290063) peak position marked "&"and the Pt phase (JCPDS card No.) peaks marked by "#" in Fig. 5. The peak due to γ-Al_2O_3 phase at 2-θ position of 39.52° and the 100% peak due to Pt phase at 39.76° can be easily resolved. We observe that the alumina sample contains a predominant amount of AlO(OH) phase. This oxy-hydroxide phase AlO(OH) commonly termed as boehmite is generally the precursor to γ-Al_2O_3 phase and completely converts to the alumina phase at higher temperatures [34–36]. The powder X-ray diffraction pattern of the used catalyst sample is quite complicated due to appearance of large number of peaks but is interesting. The powder XRD pattern of the used sample shows evidence of both the γ-Al_2O_3 and Pt phases identified in the fresh catalyst but the AlO(OH) phase disappeared. Besides, $Al_2(SO_4)_3$ phase was detected in the spent sample (peaks marked by * in Fig. 5). Thus, alumina reacts with the reactant SO_3 at high temperatures generating the aluminum sulfate phase some of which has been retained in the spent catalyst. In our investigation with iron oxide catalysts [14], metal sulfates were detected in minor amounts in the spent samples, but it decomposed at the reaction temperature. Thus, metal sulfates were proposed to be the reaction intermediates i.e. the sulfates were metastable species formed at the high reaction temperature (temperatures where the metal sulfate is supposed to decompose forming SO_2) and its formation and decomposition was the mechanism of sulfuric acid decomposition. But the $Al_2(SO_4)_3$ probably are more stable species than iron sulfates at the reaction temperatures and so does not completely decompose at the reaction temperature, and are seen prominently in the XRD pattern, a case of substrate sulfation as also noticed by Norman et al. [27]. The reactant reacts with the substrate forming stable aluminum sulfate phase. Further, many other alumina phases have been generated which prominently includes the δ-Al_2O_3, θ-Al_2O_3 and α-Al_2O_3 phases in addition to the γ-Al_2O_3 phases present in the fresh catalyst. The phase transformation of aluminas is by itself a topic of relevance and is well studied, reported and still pursued [37–40]. The detailed powder XRD investigation of the different phases of alumina has been carried out by Santos et al. [40], where it is shown that boehmite undergoes phase transformations with an increase in temperature the sequence being boehmite to gamma to delta to theta to alpha phase. Again, the phase transformation of γ-Al_2O_3 to α-Al_2O_3 was observed only above 1000 °C by Legros et al. [41,42]. But since the gamma alumina phase was exposed to vapors of sulfuric acid at 800 °C for a prolonged time period (100 h), we observed the partial formation of even α-Al_2O_3 phase. Thus prolonged use (100 h) at a temperature of ~800 °C converts the γ-Al_2O_3 and the AlO(OH) phases to other phases of alumina. Any sort of phase transformations of the support alumina might have a significant impact on the catalytic properties of alumina supported metal catalysts [43], in some cases reported as being the major cause for deactivation [44] while in others the phase of the alumina used has a major impact on catalyst stability [45].

3.2.4. FTIR results

The FTIR spectra of the fresh and the spent Pt/Al_2O_3 catalyst are shown in Fig. 6 and the results support our XRD findings. The characteristic FTIR peaks in the 500-750 cm^{-1} i.e. 621 cm^{-1} and 741 cm^{-1} are assigned to the vibrations of AlO_6 present in boehmite [34] and the 895 cm^{-1} shoulder due to the presence of γ-AlO_4 [46]. The 1072 cm^{-1} peak is due to the presence of δ (OH) in boehmite [34]. Thus, all these peaks are combined characteristic of γ-Al_2O_3 and boehmite [34]. But these peaks are not clearly visible in the spent sample suggesting a change in phase supporting our powder XRD observations. The spent catalyst on the other hand shows peaks in the 1100 cm^{-1} to 1325 cm^{-1} due the S—O stretching frequencies present in bulk and surface aluminum sulfates [47,48].

3.2.5. Morphological properties

The scanning electron micrograph images of the fresh and spent Pt/Al_2O_3 catalyst are shown in Fig. 7. The size (5 mm diameter) and the spherical shape of the catalyst granules are clearly observed. The SEM image of the fresh catalyst shows the alumina particles having very large variation both in size (100 nm to 10 μm) and shape. At some places hexagonal plates typical of γ-Al_2O_3 derived from boehmite can also be seen [49]. The grain boundaries

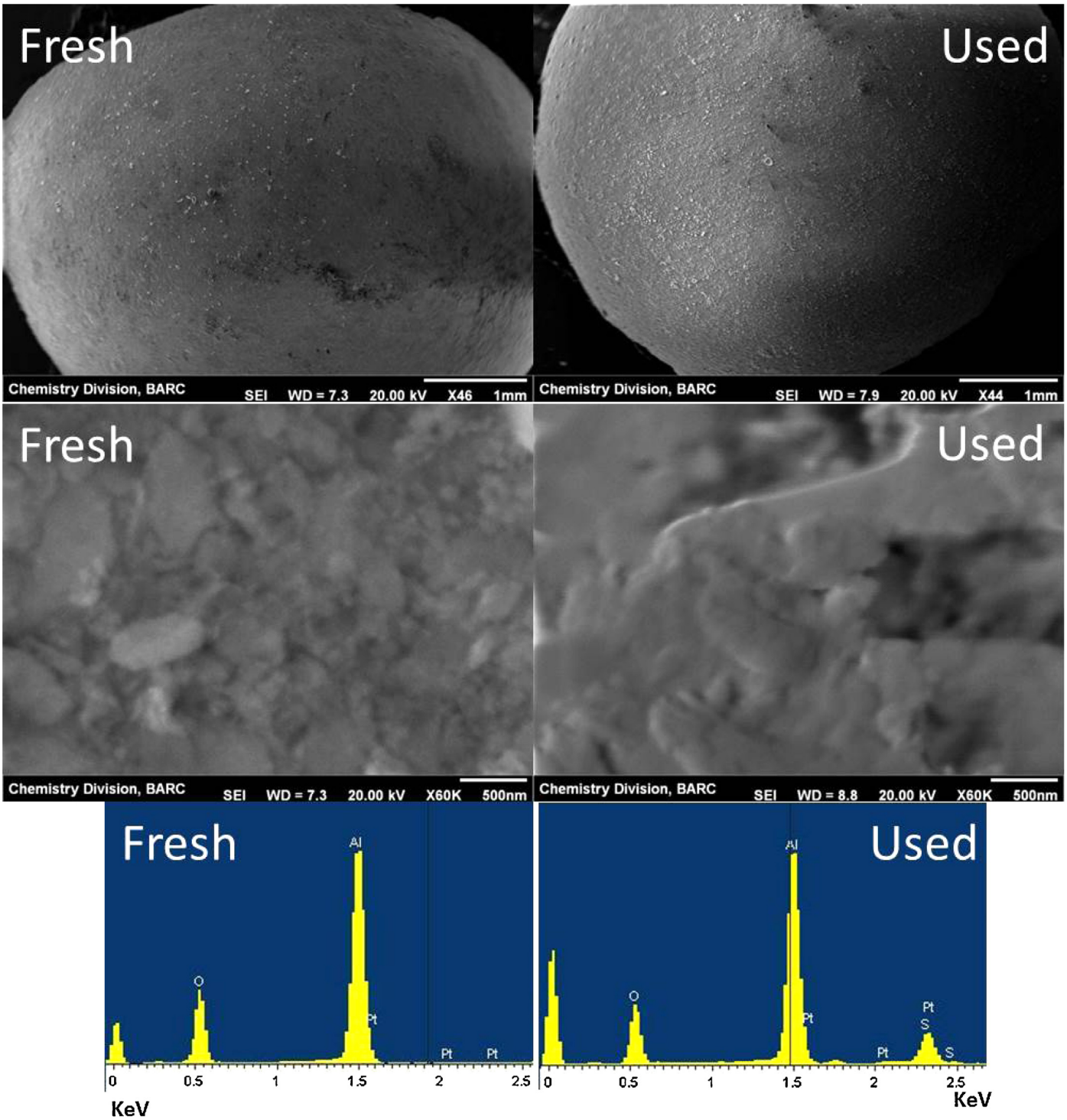

Fig. 7. SEM-EDX images of the fresh and spent of the Pt/Al_2O_3 catalyst.

are clearly visible. In contrast the spent catalyst does not exhibit clear grain boundaries and particles are not distinct. Larger aggregates are visible instead, probably due to particle agglomeration by sintering at high temperature and densification of the support alumina. This densification process causes a reduction in porosity which supports our earlier observation in the N_2 adsorption–desorption isotherms. Thus on prolonged catalytic use the microstructure of the surface undergoes major changes – sintering and densification of alumina occurs along with a reduction in porosity. The sintering and densification of porous or nanocrystalline powders is generally observed on prolonged heating at higher temperature and this topic has been studied in great details and comprehensively reviewed [50–52]. The EDX spectra of the samples are also shown in Fig. 7. The spectra indicate the presence of O, Al and Pt in the fresh catalyst while S is present additionally in the spent samples. This S obviously comes from the $Al_2(SO_4)_3$ phase detected in the spent catalyst sample.

The morphological characters of the fresh and spent Pt/Al_2O_3 catalyst samples were further evaluated by Transmission Electron Microscopy. Fig. 8 exhibits the dispersion of the Pt particles on the

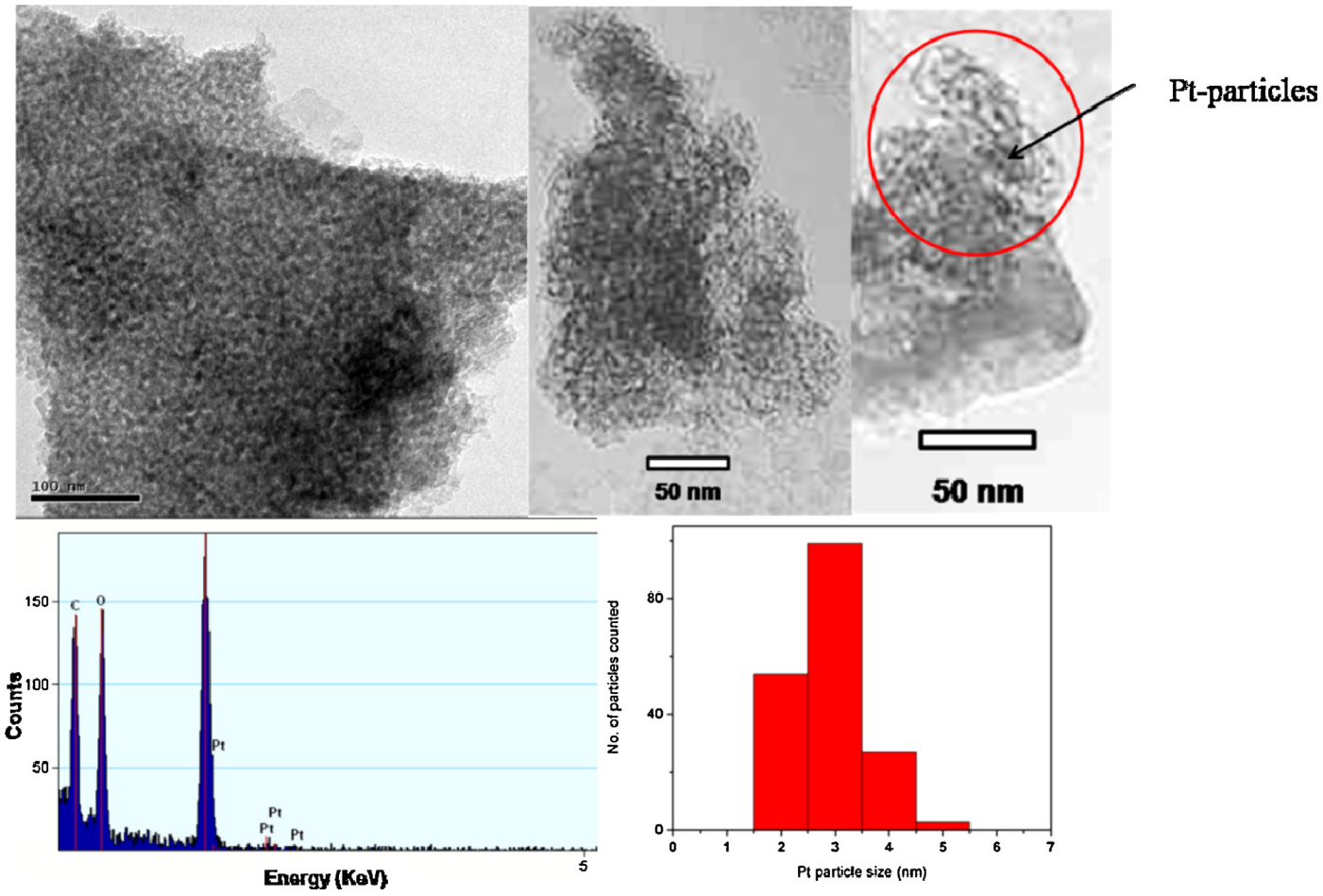

Fig. 8. TEM-EDS images of the fresh Pt/Al_2O_3 catalyst along with the particle size distribution.

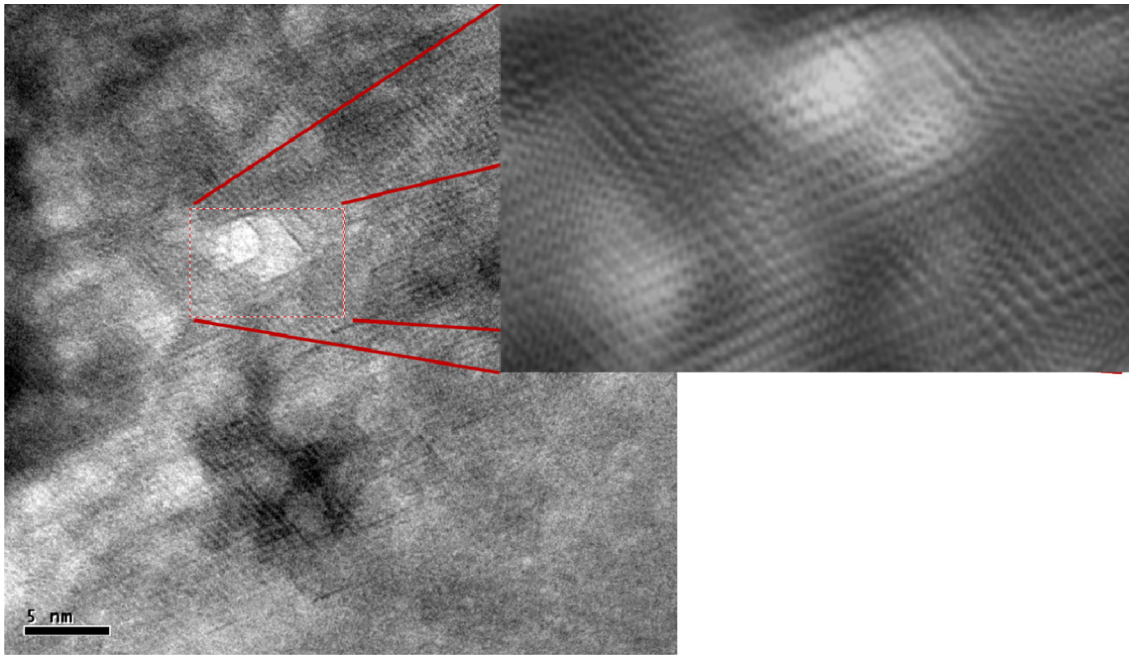

Fig. 9. HRTEM image of the fresh Pt/Al_2O_3 catalyst along with a magnified view of a selected portion.

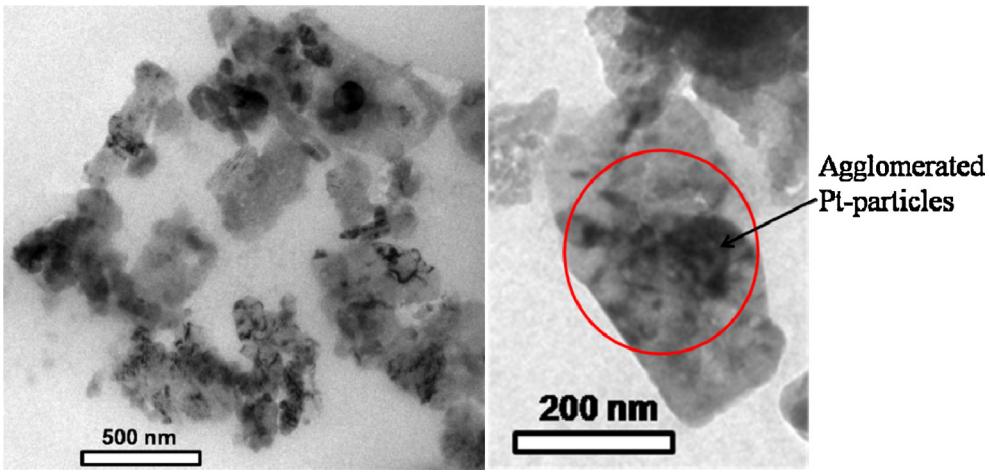

Fig. 10. TEM images of the used Pt/Al_2O_3 catalyst.

fresh commercial Pt/Al_2O_3 along with the EDS image and the particle size distribution. We can observe from the images that very fine Pt particles are uniformly distributed over the larger alumina grains. The Pt particles are highly monodisperse with crystallite size in range of ~2–3 nm as presented in the histogram of the Pt-particle size distribution (Fig. 8). The histogram shows the narrow distribution of particle size. The EDS pattern is also shown which depicts the presence of Pt. The high resolution TEM image of the fresh Pt/Al_2O_3 sample along with the magnified view of a selected portion of the HRTEM image is shown in Fig. 9. The shape and size of the Pt nano particles are more distinctly viewed from these images as also the metal-support interaction. The crystallinity of the support is visibly understood from the lattice fringes present but the lattice spacing of the Pt-particles is not clearly seen.

The morphological changes of the Pt-particles on use in sulfuric acid decomposition at high temperatures are clearly visible from the TEM images of the used catalyst samples shown in Fig. 10. The distribution of the metal over the alumina surface now becomes highly irregular. Prolonged use at high temperatures also results in metal particle agglomeration. Platinum agglomerates of varied shape and size are now non-uniformly scattered over the support grain. To strengthen this aspect further TEM images were recorded at different regions of the carbon coated copper grid on which the used sample was dispersed. One such typical result is shown in Fig. 11 where we can observe a Pt agglomerate even of the order of 80 nm. The EDS spectra show the presence of Al, Pt, O and even S. Thus, prolonged use of Pt/Al_2O_3 catalyst at elevated temperature under acidic reaction environment causes considerable sintering of the Pt particles.

4. Discussions

4.1. Physico-chemical changes of the Pt/Al_2O_3 catalyst on 100 h use

Thus the ex-situ characterization provides an insight in to the changes in physical and chemical properties of the Pt/Al_2O_3 catalyst granules due to prolonged (100 h) use for sulfuric acid decomposition reaction under harsh reaction environment (high temperature, steam, corrosive oxides of sulfur and oxygen). The surface area of the catalyst decreases and also we observed a decrease in H_2 uptake by the active metal Pt in pulsed chemisorption experiments. A reduction in porosity of the support was observed both by nitrogen adsorption desorption isotherm and SEM. Aluminum sulfate stable phase was detected in the powder X-ray diffraction pattern of the spent catalyst which was further verified by FTIR results. Also, the substrate alumina underwent phase changes on prolonged use with several new phases appearing in the used catalyst. Finally, considerable agglomeration of the platinum metal particles was observed from the TEM images. Thus, surface area reduction, substrate sulfation, substrate phase transformation, porosity loss and metal particle agglomeration are the major physicochemical changes observed for Pt/Al_2O_3 catalyst on prolonged use for the sulfuric acid decomposition reaction at 800 °C for 100 h.

4.2. Role of Pt and Al_2O_3 on reaction mechanism

Among the above identified factors, metal particle agglomeration and loss in active metal dispersion is expected to affect the catalytic activity more severely as the reaction has been reported to proceed via the adsorption and decomposition of molecular SO_3 through the intermediate formation of adduct $[SO_2{\cdot}O]$ on the noble metal sites [53]. But, the catalytic activity was still reasonably high as compared to the very low percentage metal dispersion observed experimentally. The low dispersion might be due to two factors – one because of the metal particle agglomeration and their consequent growth and secondly due to the platinum particles being covered by the aluminum sulfate formed and thus not available on the surface. This sort of phenomenon was also evident in SO_2 poisoning studies on Ru/Al_2O_3 during preferential CO oxidation, where, Ru particles were found to remain covered by sulfur oxides on support and thus were unavailable for reaction [54]. If, the very low dispersion was solely due to the first factor then definitely the SO_2 yield would have decreased drastically and should not have retained the ~73% SO_2 yield even after 100 h. But, if the metal dispersion was so low due to the second factor then we might expect a reasonable catalytic activity only if a synergy existed between the metal and the modified support i.e. an interaction between platinum particles and aluminum sulfate. To investigate this fact, the spent catalyst was subjected to TG-DTG in the temperature range of 40–1100 °C and the evolved gases were analyzed by FTIR. Bulk aluminum sulfate and a mixture of aluminum sulfate and Al_2O_3 (1:4 by weight) were separately investigated under similar conditions. The DTG profiles of all the three samples are plotted as a function of temperature in Fig. 12. The low temperature peaks in Fig. 12 are due to loss of water while the high temperature peaks (>500 °C) are due to the decomposition of sulfates. The bulk aluminum sulfate and the aluminum sulfate in the mechanical mixture in Al_2O_3 undergoes decomposition in one step and at a much higher temperature (decomposition onset at 650 °C and 665 °C respectively) as compared to the sulfate present on the used Pt/Al_2O_3 catalyst, which undergoes a two-step decomposition and at a lower temperature

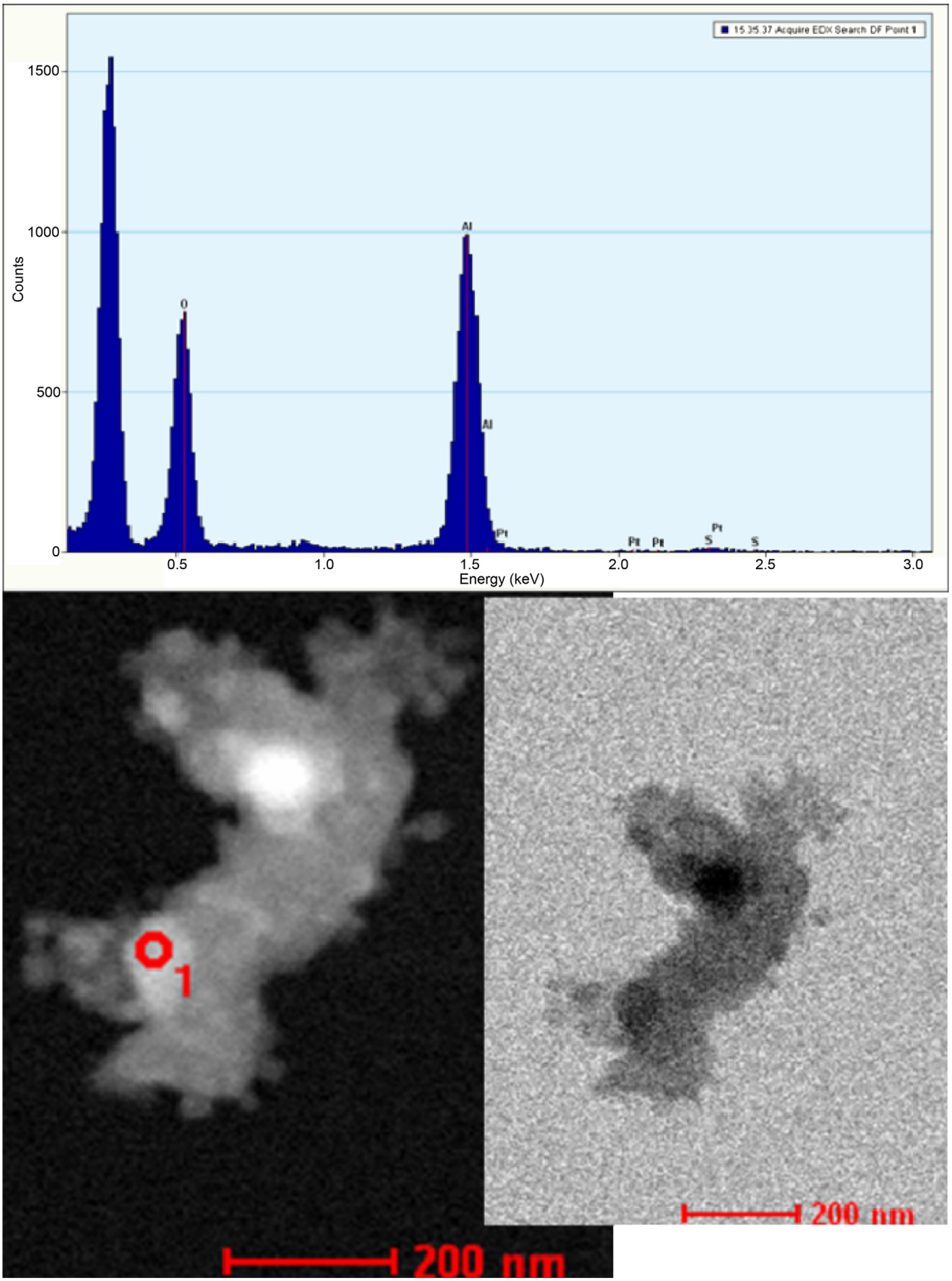

Fig. 11. Dark and bright field TEM image of a chosen grain of the used Pt/Al_2O_3 catalyst along with EDS of a selected region (O_1) showing Pt- particles of size of 80 nm.

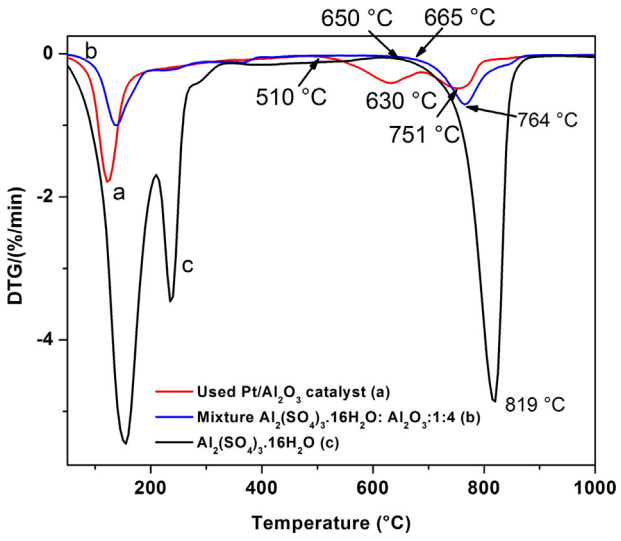

Fig. 12. Comparison of the DTG profiles of the spent Pt/Al_2O_3 catalysts (a) with a 1:4 molar mixture of $Al_2(SO_4)_3$ with Al_2O_3 (b) and $Al_2(SO_4)_3$ (c).

(onset at 510 °C). Further, the ratio of the area under the peak, of the first (peak having maxima at 630 °C) and second peak (maxima at 751 °C) was found to be 1:2. This suggests that, in presence of Pt the decomposition of $Al_2(SO_4)_3$ to Al_2O_3 proceeds via aluminum oxysulfate species involving following two steps [55]:

$$Al_2(SO_4)_3 \rightarrow Al_2O(SO_4)_2 + SO_2 + \tfrac{1}{2}O_2 \quad (3)$$

$$Al_2O(SO_4)_2 \rightarrow Al_2O_3 + 2SO_2 + O_2 \quad (4)$$

Alteration in the decomposition pattern of aluminum sulfate present on spent Pt/Al_2O_3 catalyst in comparison to bulk aluminum sulfate both in terms of reduction in decomposition temperature and modification of decomposition profile can be seen from Fig. 12. SO_2 was evolved as the decomposition product in all the cases which were analyzed by FTIR with the peak maxima of the DTG curve being ~630 °C and 751 °C from sulfate in spent catalyst in sharp contrast to ~819 °C observed for bulk aluminum sulfate. Thus the decomposition temperature of aluminum sulfate is found to be significantly lowered in presence of platinum. Metal-support interaction appears to play a crucial role in this phenomenon and the metal-support (in modified sulfate form) might work in synergism in the mechanism of sulfuric acid decomposition reaction over Pt/Al_2O_3 catalyst. It can now be inferred that the support plays an active role in the decomposition mechanism in presence of platinum and participates in the reaction as a sulfate intermediate. In addition to the SO_3 adsorption-decomposition mechanism on Pt suggested elsewhere [53], the SO_3 might bind to the alumina forming aluminum sulfate, which at the reaction temperature (800 °C), are sufficiently facile in presence of platinum, to be decomposed into alumina and SO_2 the reaction product. Thus an alternative pathway to the decomposition mechanism can be proposed which involves the aluminum sulfate formation and its decomposition in presence of platinum. It could be proposed that the operation of this alternative mechanism might support the phenomenon of maintenance of reasonable SO_2 yield even after 100 h when the metal dispersion has been bought to a bare minimum. The, loss in metal dispersion is probably due to the platinum particles being covered by the newly formed aluminum sulfate phase and thus not available for H_2 adsorption in the pulsed chemisorption experiments [54]. But, this loss in dispersion does not completely inhibit the progress of the reaction as according to our hypothesis the reaction can now also proceed via aluminum sulfate formation and decomposition in addition to the adsorption-decomposition mechanism. A synergy between the Pt particles and the modified support (sulfated alumina) might play a crucial role in sustaining the catalytic activity of Pt/Al_2O_3 catalyst during prolonged use for sulfuric acid decomposition reaction.

5. Conclusion

In this study we conclude that 20 g of commercial Pt (~0.5 wt. %)/Al_2O_3 granules (4–6 mm diameter) were successfully employed as catalysts for sulfuric acid decomposition reaction, the most endothermic step of Sulfur–Iodine thermochemical cycle. The SO_2 yield increased with the increase in temperature for the Pt/Al_2O_3 granules at a WHSV of ~3.4 g acid g^{-1} h^{-1} with the maximum reaching to ~83% at 825 °C. In a typical 100 h catalytic run at 800 °C and a WHSV of ~3.4 g acid g^{-1} h^{-1}, the Pt/Al_2O_3 catalyst suffered a decrease in SO_2 yield from 80% to 73%. To investigate the probable cause for this decrease both the fresh and the spent catalyst were analyzed for changes in structure and morphology by various techniques. Reduction in N_2-BET-surface area, alumina substrate sulfation, alumina partial phase transformation, reduction in porosity of support alumina, and metal particle agglomeration (drastic loss in metal dispersion) are the major physicochemical changes observed for Pt/Al_2O_3 catalyst due to use in the sulfuric acid decomposition reaction at 800 °C for 100 h. Synergy between the Pt metal and the modified support (sulfated alumina) was established.

Acknowledgements

The authors acknowledge N. Manoj of Chemistry Division for recording the SEM images, HWD, BARC for recording the N_2 adsorption isotherms and pulsed chemisorption experiments. This work was partially funded by Department of Science and Technology (DST) New Delhi (No. DST/TSG/SH/2011/106).

References

[1] C.E. Bamberger, D.M. Richardson, Cryogenics 16 (1976) 197–208.
[2] M.A. Pena, J.P. Gomez, J.L.G. Fierro, Appl. Catal. A: Gen. 144 (1996) 7–57.
[3] P. Favuzza, C. Felici, L. Nardi, P. Tarquini, A. Tito, Appl. Catal. B: Environ. 105 (2011) 30–40.
[4] K. Onuki, S. Kubo, A. Terada, N. Sakaba, R. Hino, Energ. Environ. Sci. 2 (2009) 491–497.
[5] S. Kubo, H. Nakajima, S. Kasahara, S. Higashi, T. Masaki, H. Abe, K. Onuki, Nucl. Engg. Des. 233 (2004) 347–354.
[6] S. Brutti, G. De Maria, G. Cerri, A. Giovannelli, B. Brunetti, P. Cafarelli, E. Semprin, V. Barbarossa, A. Ceroli, Int. J. Hydrogen Energ. 31 (2006) 883–890.
[7] P. Cafarelli, E. Semprin, V. Barbarossa, A. Ceroli, Ind. Engg. Chem. Res. 20 (2007) 6393–6400.
[8] L.E. Brecher, S. Spewock, C.J. Warde, Int. J. Hydrogen Energ. 2 (1977) 7–15.
[9] G.E. Beghi, Int. J. Hydrogen Energ. 11 (1986) 761–771.
[10] J. Leybros, A. Saturnin, C. Mansilla, T. Gilardi, P. Carles, Int. J. Hydrogen Energ. 35 (2010) 1019–1028.
[11] J. Leybros, T. Gilardi, A. Saturnin, C. Mansilla, P. Carles, Int. J. Hydrogen Energ. 35 (2010) 1008–1018.
[12] A.M. Banerjee, M.R. Pai, K. Bhattacharya, A.K. Tripathi, V.S. Kamble, S.R. Bharadwaj, S.K. Kulshreshtha, Int. J. Hydrogen Energ. 33 (2008) 319–326.
[13] A.M. Banerjee, M.R. Pai, S.S. Meena, A.K. Tripathi, S.R. Bharadwaj, Int. J. Hydrogen Energ. 36 (2010) 4768–4780.
[14] A.M. Banerjee, A.R. Shirole, M.R. Pai, A.K. Tripathi, S.R. Bharadwaj, D. Das, P.K. Sinha, Appl. Catal. B: Environ. 127 (2012) 36–46.
[15] L.N. Yannopoulos, J.F. Pierre, Int. J. Hydrogen Energ. 9 (1984) 383–390.
[16] T.-H. Kim, G.-T. Gong, B.G. Lee, K.-Y. Lee, H.-Y. Jeon, C.-H. Shin, H. Kim, K.D. Jung, Appl. Catal. A: Gen. 305 (2006) 39–45.
[17] D.M. Ginosar, H.W. Rollins, L.M. Petkovic, K.C. Burch, M.J. Rush, Int. J. Hydrogen Energ. 34 (2009) 4065–4073.
[18] M. Machida, Y. Miyazaki, Y. Matsunaga, K. Ikeue, Chem. Commun. 47 (2011) 9591–9593.
[19] G. Karagiannakis, C.C. Agrafiotis, A. Zygogianni, C. Pagkoura, A.G. Konstandopoulos, Int. J. Hydrogen Energ. 36 (2011) 2831–2844.
[20] A. Giaconia, S. Sau, C. Felici, P. Tarquini, G. Karagiannakis, C. Pagkoura, C. Agrafiotis, A.G. Konstandopoulosc, D. Thomey, L. de Oliveira, M. Roeb, C. Sattler, Int. J. Hydrogen Energ. 36 (2011) 6496–6509.
[21] G. Karagiannakis, C.C. Agrafiotis, C. Pagkoura, A.G. Konstandopoulos, D. Thomey, L. de Oliveira, M. Roeb, C. Sattler, Int. J. Hydrogen Energ. 37 (2012) 8190–8203.

[22] V. Barbarossa, S. Bruttib, M. Diamantia, S. Saua, G. De Mariab, Int. J. Hydrogen Energ. 31 (2006) 883–890.
[23] M. Masato, K. Takahiro, Y. Hiroaki, T. Tonami, J. Phys. Chem. C 117 (2013) 26710–26715.
[24] S.J. Tauster, S.C. Fung, R.T.K. Baker, J.A. Horsley, Science 211 (1981) 1121–1125.
[25] L.F. Liotta, Appl. Catal. B: Environ. 100 (2010) 403–412.
[26] J. Cooper, J. Beecham, Platin. Met. Rev. 57 (2013) 281–288.
[27] J.H. Norman, K.J. Mysels, R. Sharp, D. Williamson, Int. J. Hydrogen Energ. 7 (1982) 545–556.
[28] D.M. Ginosar, L.M. Petkovic, A.W. Glenn, K.C. Burch, Int. J. Hydrogen Energ. 32 (2007) 482–488.
[29] L.M. Petkovic, D.M. Ginosar, H.W. Rollins, K.C. Burch, P.J. Pinhero, H.H. Farrell, Appl. Catal. A: Gen. 338 (2008) 27–36.
[30] B.M. Nagaraja, K.D. Jung, B.S. Ahn, H. Abimanyu, K.S. Yoo, Ind. Eng. Chem. Res. 48 (2009) 1451–1457.
[31] L.S. Young, J. Heon, K.W. Joo, S.Y. Gun, J. Kwang-Deog, Int. J. Hydrogen Energ. 38 (2013) 6205–6209.
[32] S.N. Rashkeev, D.M. Ginosar, L.M. Petkovic, H.H. Farrell, Catal. Today 139 (4) (2009) 291–298.
[33] H. Tagawa, T. Endo, Int. J. Hydrogen Energ. 14 (1989) 11–17.
[34] S.-M. Kim, Y.-J. Lee, J.W. Bae, H.S. Potdar, Appl. Catal. A: Gen. 348 (2008) 113–120.
[35] R. Vidruk, M.V. Landau, M. Herskowitz, V. Ezersky, A. Goldbourt, J. Catal. 282 (2011) 215–227.
[36] Y. Liu, F.-Y. Huang, J.-M. Li, W.-Z. Weng, C.-R. Luo, M.-L. Wang, W.-S. Xia, C.-J. Huang, H.-L. Wan, J. Catal. 256 (2008) 192–203.
[37] Y. Wang, K. Shih, X. Jiang, Ceram. Int. 38 (2012) 1879–1886.
[38] R.S. Zhou, R.L. Snyder, Acta Crystallogr. B 47 (1991) 617–630.
[39] Y. Wang, C. Suryanarayana, J. Am. Ceram. Soc. 88 (2005) 780–783.
[40] P. Souza Santos, H. Souza Santos, S.P. Toledo, Mater. Res. 3 (4) (2000) 104–114.
[41] C. Legros, C. Carry, P. Bowen, H. Hofmann, J. Eur. Ceram. Soc. 19 (1999) 1967.
[42] C. Legros, F. Herbst, S. Lartigue-Korinek, C. Carry, P. Bowen, Rev. Metall. 99 (2002) 1073.
[43] N. Jiang, K.S.R. Rao, M.-J. Jin, S.-E. Park, Appl. Catal. A Gen. 425–426 (2012) 62–67.
[44] S.-J. Park, J.W. Bae, G.-I. Jung, K.-S. Ha, K.-W. Jun, Y.-J. Lee, H.-G. Park, Appl. Catal. A: Gen. 413–414 (2012) 310–321.
[45] M.G. Álvarez, M. Plísková, A.M. Segarra, F. Medina, F. Figueras, Appl. Catal. B: Environ. 113–114 (2012) 212–220.
[46] G.K. Priya, P. Padmaja, K.G.K. Warrier, A.D. Damodaran, G. Aruldhas, J. Mater. Sci. Lett. 16 (1997) 1584–1587.
[47] H. Abdulhamida, E. Fridell, J. Dawodya, M. Skoglundha, J. Catal (2006) 200–210.
[48] G. Corro, J.L.G. Fierro, V.C. Odilon, Catal. Commun. 4 (2003) 371–376.
[49] P. Souza Santos, H. Souza Santos, S.P. Toledo, Mater. Res. 3 (2000) 104–114.
[50] M.N. Rahaman, Ceramic Processing and Sintering, Marcel Dekker, New York, 2003.
[51] S.-J.L. Kang, Sintering, Densification, Grain Growth and Microstructure, Elsevier, Amsterdam, 2005.
[52] R. Haim, M. Levin, A. Shlayer, C. Estournes, Adv. Appl. Ceram. 107 (2008) 159.
[53] G. I. Golodates Heterogeneous catalytic reaction involving molecular oxygen. Elsevier Science Publisher.
[54] H. Wakita, Y. Kani, K. Ukai, T. Tomizawa, T.W. Takeguchi, Ueda Appl. Catal. A: Gen. 283 (2005) 53–61.
[55] Y. Pelovski, V. Petkova, J. Therm. Anal. 49 (1997) 1227–1241.